

# Establishing a core microbiome in acetate-fed microbial fuel cells

Keaton Larson Lesnik · Hong Liu

Received: 14 September 2013 / Revised: 19 December 2013 / Accepted: 24 December 2013 / Published online: 9 January 2014  
© Springer-Verlag Berlin Heidelberg 2014

**Abstract** Establishing a core microbiome is the first step in understanding and subsequently optimizing microbial interactions in anodic biofilms of microbial fuel cells (MFCs) for increased power, efficiency, and decreased start-up times. In the present study, we used 454 pyrosequencing to demonstrate that a core anodic community would consistently emerge over a period of 4 years given similar conditions. The development and variation across reactor designs of these communities was also explored. The core members present in all high-power generating biofilms were *Geobacter*, *Aminiphilus*, *Sedimentibacter*, *Acetoanaerobium*, and *Spirochaeta*, accounting for 72±9 % of all genera. *Aminiphilus* spp., member of the Synergistetes phylum was present at higher abundances than previously reported in any other ecological studies. Results suggest a stable core microbiome in acetate-fed MFCs on both phylogenetic and functional levels.

**Keywords** Microbial fuel cell · 454 pyrosequencing · Core microbiome · Community analysis · Cloth-electrode assembly

## Introduction

Microbial electrochemical systems such as microbial fuel cells (MFCs) are capable of harnessing microbial metabolism to catalyze redox reactions in electrochemical cells. In MFCs, the electron transfer to an anodic electrode is linked to the oxidation of organic substrates (Logan 2008). This release of electrical energy accompanying the degradation of organic compounds was first reported in 1911, but recent years have seen an increased focus on the development of technologies to

take advantage of this phenomenon for applications in wastewater treatment and alternative energy generation (Franks and Nevin 2010; Potter 1911).

Low electrical current outputs have previously limited commercial applications, yet recent advances have made MFC technology increasingly feasible and several scale-up operations are underway. The highest recorded volumetric power densities (2.87 kW m<sup>-3</sup>) have been reported recently utilizing a novel cloth-electrode assembly (CEA) MFC design (Fan et al. 2012). High-power outputs such as these have suggested great potential for use of MFC technologies for practical applications, all made possible by microorganisms that are exceptionally efficient at converting energy stored in organic compounds into electricity.

Pure cultures of bacteria such as *Geobacter sulfurreducens* have been shown to produce current densities as high as 7.1 A m<sup>-2</sup> using an “H-cell” design with solid graphite electrodes though the biocatalytic capacity for power production in mixed consortia is generally about twice that of pure cultures of *G. sulfurreducens* (Ishii et al. 2008; Yi et al. 2009). Mixed species biofilms have been able to generate current densities of 12.7 and 26.2 A m<sup>-2</sup>, while also offering advantages in stability, substrate flexibility, and culture maintenance costs (Borole et al. 2011; Fan et al. 2008). Because of these advantages, mixed communities are often used for wastewater treatment applications and MFC anodes may be colonized by a wide variety of microorganisms (Kiely et al. 2011; Logan 2008).

Through the use of techniques such as pyrosequencing of the variable regions of 16S rRNA genes, MFC anode communities have been found to be diverse yet uneven, oftentimes dominated by a small percentage of the species present even when compared to related wastewater treatment systems (Wang et al. 2012). Well characterized exoelectrogens such as *Geobacter* spp. are often predominant in acetate-fed MFCs capable of composing upwards of 60 % of anodic biofilms

K. L. Lesnik · H. Liu (✉)  
Department of Biological and Ecological Engineering, Oregon State  
University, Corvallis, OR 97333, USA  
e-mail: liuh@enr.orst.edu

though high-power communities with a low abundance (14 %) or an absence of *Geobacter* spp. have been reported (Borole et al. 2011; Kiely et al. 2010; Malvankar et al. 2012). These communities present a measure of stability, as anodic biofilm communities inoculated from different sources have been reported to converge over a period of 2 months, producing roughly equivalent power (Yates et al. 2012). In contrast, biofilms formed from the same inoculum on dissimilar anode designs (planar carbon cloth anodes vs. volumetric graphite brush anodes) have displayed differences in community structure (Vargas et al. 2013). MFC anode community studies have yet to address the presence and function of many commonly occurring phylogenies along with the long-term consistency and stability of these communities (Lee et al. 2010; Yates et al. 2012; Zhang et al. 2012).

In the present study, we analyze the core microbiome of high-power acetate-fed MFC anodes over a long duration in order to begin to establish more definite linkages between reactor performance, design, community composition, stability, and consistency with the goal of ultimately optimizing for increased power/efficiency as well as decreased start-up times. This was done through comparison of high-power communities that developed consistently over a period of 4 years in commonly used single chamber air-cathode (SC) MFC reactors (Liu and Logan 2004). SC-MFC communities were then compared to those from CEA-MFCs to determine core community conservation across reactor designs. The effect of increased oxygen exposure and development of these communities during start-up was also explored.

## Materials and methods

### Microbial fuel cell design and operation

MFC designs used in this study were SC-MFCs and CEA-MFCs both previously described (Fan et al. 2012; Liu and Logan 2004). The original inoculum used to seed the first MFC reactors was collected from domestic wastewater (Corvallis Wastewater Treatment Plant, Corvallis, OR) in 2006 with subsequent cultures from active MFCs fed with acetate. Communities labeled MFC08, MFC10, and MFC12 were all from identical 12 ml SCAC-MFCs operated in batch mode and sampled in 2008, 2010, and 2012, respectively, after operation for at least 1 month and stable power outputs of at least  $0.8 \text{ W m}^{-2}$ . Communities labeled CEA1 and CEA2 were from CEA-MFC reactors operated in continuous flow mode for 2 months; the main difference between the reactors was that the design of CEA1 reactor had one third the liquid volume of CEA2 (30 vs. 90 ml). Media used in all experiments was a Modified *Geobacter* Medium (pH 7) that consisted of the following (per liter): KCl, 0.13 g;  $\text{NaH}_2\text{PO}_4 \cdot \text{H}_2\text{O}$ , 5.84 g;

$\text{Na}_2\text{HPO}_4 \cdot 7\text{H}_2\text{O}$ , 15.5 g; vitamin, 12.5 mL; and mineral, 12.5 mL solution as previously reported (Fan et al. 2007). Sodium acetate was used as the electron donor in both CEA (100 mM) and SC-MFC (60 mM) reactors with concentrations optimized for power generation. High concentrations of sodium acetate (100 mM) used in continuous flow reactors resulted in substrate inhibition in batch-mode reactors; therefore, concentrations were decreased to 60 mM in SC-MFCs. Ammonium concentrations were also optimized with  $0.31 \text{ g l}^{-1}$  of  $\text{NH}_4\text{Cl}$  used for SC-MFC media and  $1.5 \text{ g l}^{-1}$  for CEA reactor media. SC-MFCs were considered stable once voltages were repeatable over three batches. At this point, resistances were changed until voltage stabilized and power densities were calculated. CEA-MFC voltage outputs generally took a week to stabilize, and maximum power output was determined using the same procedure.

Effluent from high-power MFCs was used as the inoculum to seed other MFCs, and the development of these communities was investigated by analyzing total microbial diversity (combined planktonic effluent and biofilm communities) over 2 weeks. CCom1 represents the total diversity of a mature, stable, high-power MFC at day 1; the effluent from which was removed and introduced into a new reactor at day 0. EffMFC represents the day 0 community. CCom2 is the community at the midpoint of development (day 7), and CCom3 is the reemergence of a stable high-power MFC at day 14. The community-labeled AirMFC was exposed to increased oxygen by pumping air into the MFC at  $1.0 \text{ ml min}^{-1}$  for 2 weeks.

### Sample collection and DNA extraction

All SC-MFC biofilms samples (MFC08, MFC10, MFC12, and AirMFC) were collected in the same manner; the  $7 \text{ cm}^2$  carbon cloth anode was removed, placed in a sterile 50 ml tube with 10 ml of 100 mM phosphate buffered saline (PBS), and 5 ml of 2 mm sterile glass beads. Tubes were then vortexed 5 min to remove the biofilm from the anode. Subsequently, cells were concentrated by centrifugation. The CEA-MFC biofilm samples (CEA1 and CEA2) were collected in a similar manner except a larger  $100 \text{ cm}^2$  section of the carbon cloth anode was used. For the biofilm and effluent community samples (CCom1-3), 10 ml of the effluent was added to the tube instead of PBS. No carbon cloth anode was used to collect the effluent community sample (EffMFC); 10 ml of the effluent solution from the MFC was withdrawn and cells centrifuged. DNA extraction was performed using a Qiagen Blood and Tissue DNA extraction kit (Valencia, CA). The quality of the DNA extraction was checked on an agarose gel which was further verified through use of spectrophotometer (NanoDrop, Wilmington, DE, USA).

## Amplicon library construction and 454 pyrosequencing

DNA from each community was amplified using a set of primers developed by the Ribosomal Database Project (RDP) that targets the hyper-variable V4 region of the 16S rRNA gene (Cole et al. 2009). The 454 adapter sequence (5'-3') CCTATCCCCTGTGTGCCTTGGCAGTC was followed by a 8-bp long multiplex identifier (MID) unique to each sample and then the forward primer AYTGGGYDTAAA GNG (*Escherichia coli* position 563-577). The reverse primers were composed of the adapter sequence followed by the reverse primer sequence, CCGTCAATTCMTTTRAGT (*E. coli* 907-924). Twenty-five microliter PCR reaction volumes were used for optimization followed by 50  $\mu$ l amplification reactions. A high-fidelity Taq polymerase (Invitrogen Platinum) was used with along with MgSO<sub>4</sub> (2.5 mM), vendor supplied buffer, BSA (0.1 mg/ml), dNTPs (250  $\mu$ M), and primers (1  $\mu$ M). An initial 3-min step at 95 °C was followed by 27 cycles of 95 °C (45 s), 57 °C (45 s), and 72 °C (1 min) with a final 3 min extension at 72 °C. PCR products were agarose gel purified (2 % metaphor in TAE) and bands were extracted with a QIAquick Gel Extraction Kit (Qiagen, Valencia, CA). Gel extracted material was further purified with a Qiagen PCR Cleanup kit and AMPure XP magnetic beads. Quantification of purified PCR product was performed using a Qubit fluorometer (Invitrogen, Carlsbad, CA) and qPCR (ABI PRISM 7500 FAST Detection System). Following quantification, libraries were pooled into equimolar amounts. Emulsion PCR and sequencing was performed on a 454 GS Junior pyrosequencer (Roche, Nutley, NJ, USA) at the Center for Genome Research and Biocomputing (CGRB), Oregon State University using titanium reagents and procedures consistent with protocols for unidirectional amplicon sequencing.

## Sequence and statistical analysis

The quality filtering of the pyrosequencing run was performed using the GS Run Processor (Roche). This process removed all the low quality and failed reads in addition to trimming all adaptor sequences. The Newbler assembler (Roche) was then used to group sequences based on respective MID tags. Multiple sequence alignments were performed through the use of MUSCLE with subsequent processing done through the RDP pyrosequencing pipeline (Cole et al. 2009; Edgar 2004). The aligned high-quality sequences were then taxonomically identified using the RDP Classifier tool at an 80 % confidence level. Classifier results were then used for analysis of similarities and differences between samples. Core microbiome tables (Tables 2 and 3) were generated from a random sample of 3,000 sequences from each high-power biofilm samples (MFC08, MFC10, MFC12, CEA1, and CEA2) which were then merged into their respective design groups. Subsamples and merged groups were generated

through use of MOTHUR, which was also used for clustering at a 3 % cutoff value (Schloss et al. 2009). Clustered files were used to generate rarefaction curves as well as Shannon index, Chao 1, Simpson index, and Simpson evenness values. Representative sequences of the largest clusters were selected from clustered files and entered into the Basic Local Alignment Search Tool nucleotide database to determine closest sequence matches (Altschul et al. 1990). Principle component analysis and *P* tests were performed using the Unifrac suite (Hamady et al. 2010).

## Data deposition

Metagenomic datasets were deposited in the NCBI sequence read archive under accession number SRR966001. The metagenomic project can also be accessed in NCBI under Genome Project ID 1076179 (accession PRJNA56113, <http://www.ncbi.nlm.nih.gov/bioproject?term=PRJNA56113>).

## Results

### Pyrosequencing

A unidirectional sequencing approach of ten pooled 16S rRNA gene amplicon libraries yielded a total of 120,000 reads with 112,000 key pass reads and over 44,000 reads that passed the 454 software internal quality filters. The number of quality reads per sample ranged from 2,916 to 10,361 (Table 1) with an average number of 4,438 reads per sample. While the number of quality sequences obtained is less than what is achievable using this system, 3,000 reads are more than sufficient to establish differences and similarities between communities (Kuczynski et al. 2010). Over 90 % of these reads could be identified on the phylum level with taxonomic assignments dropping to 87 % for class, 86 % for order, 83 % for family, and 73 % for genus.

### Consistency and stability of SC-MFCs

All three SC-MFC communities though started years apart and operated for different periods of time were composed primarily of the same three phyla; Proteobacteria, Firmicutes, and Synergistetes. These three phyla compose 94 % (MFC08), 85 % (MFC10), and 99 % (MFC12) of SC-MFC biofilms (Fig. 1). Though all three were highly represented, percentages of each phylum varied between samples. Proteobacteria made up 19–47 % of the biofilm while Firmicutes composed 17–57 % of the biofilm. Averaging the three samples resulted in Proteobacteria, Firmicutes, and Synergistetes percentages of 33 $\pm$ 14, 25 $\pm$ 20, and 31 $\pm$ 16 %, respectively, combining to average 92 $\pm$ 6 % of the biofilm.

**Table 1** Diversity and richness of MFC anodic communities

	Sample name	Power (W m <sup>-2</sup> )	No. of reads	No. of OTUs	Chao-1	Shannon	Simpson	S. evenness
MFCs	MFC08	0.8–1.1 <sup>a</sup>	3,156	306	674	3.71	0.06	0.05
	MFC10	0.8–1.1 <sup>a</sup>	3,069	459	1,055	4.26	0.03	0.06
	MFC12	0.9	4,252	348	701	3.49	0.07	0.04
	Total	–	10,477	933	1,983	4.41	0.03	0.03
	Average	0.9	3,492	371	810	3.82	0.05	0.05
CEAs	CEA1	4.3	3,699	405	694	3.85	0.05	0.05
	CEA2	3.4	3,722	106	145	2.82	0.10	0.10
	Total	–	7,421	476	803	3.98	0.03	0.06
	Average	3.9	3,711	256	420	3.34	0.07	0.07
Misc.	CCom1 (Day -1)	0.9	4,999	440	849	4.37	0.02	0.09
	CCom2 (Day 7)	0.4	3,214	177	282	3.76	0.03	0.16
	CCom3 (Day 14)	0.9	4,996	438	847	4.23	0.02	0.08
	EffMFC (Day 0)	–	2,916	383	693	4.17	0.03	0.08
	Air MFC	0.0	10,361	502	921	4.10	0.03	0.07
	Total (All)	–	44,384	1,797	3,578	5.22	0.01	0.05
	Average (All)	–	4,438	356	686	3.88	0.04	0.08

<sup>a</sup> Range of reported power densities from selected time period

The next most common phyla represented were Bacteroidetes (6±5 %) and Spirochaetes (2±1 %).

Genera present in SC-MFC anodic biofilms were also conserved over the period of 4 years between sampling (Fig. 2). These genera represented 86±5 % of SC-MFC biofilms and included *Geobacter* (26±14 %), *Aminiphilus* (26±20 %), *Fusibacter* (14±16 %), *Sedimentibacter* (9±6 %), *Acetoanaerobium* (6±3 %), and *Spirochaeta* (4±5 %). Representative sequences of *Geobacter* had over 99 % sequence identity to a large number of uncultured *Geobacter* clones associated with mixed cultures of microbial electrochemical systems. Representative sequence of *Aminiphilus* had a 100 % sequence identity match to *Aminiphilus circumscriptus* strain ILE-2 (NCBI Accession: NR 043061).

All members that were present at over 0.5 % of total reads are detailed in Table 2.

A few of the numerically dominant genera (*Geobacter*, *Aminiphilus*, and *Fusibacter*) each had a single time point in which the relative abundance is significantly increased or decreased. The MFC12 community had a relative abundance of *Aminiphilus* of only 3 % compared to 36 % (MFC08) and 40 % (MFC10) at the other two time points. This decrease of *Aminiphilus* was accompanied by a large increase of *Fusibacter*. Similarly, a decrease in *Geobacter* in MFC10 was linked to an increase in *Spirochaeta*. However, these differences did not appear to affect power outputs, and comparisons of differences in operational taxonomic units (OTUs) present in each assemblage show no statistical significance

**Fig. 1** Relative distribution of phyla across all high-power MFCs. MFC08, MFC10, and MFC12 represent communities in SC-MFC reactors from 2008, 2010, to 2012, respectively. CEA1 and CEA2 represent communities in two different CEA-MFC reactors from 2012. Air MFC represents a SC-MFC community exposed to increased airflow

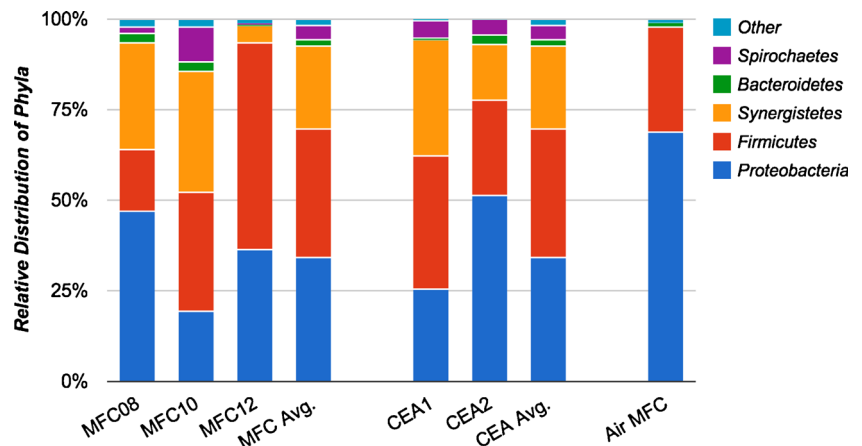
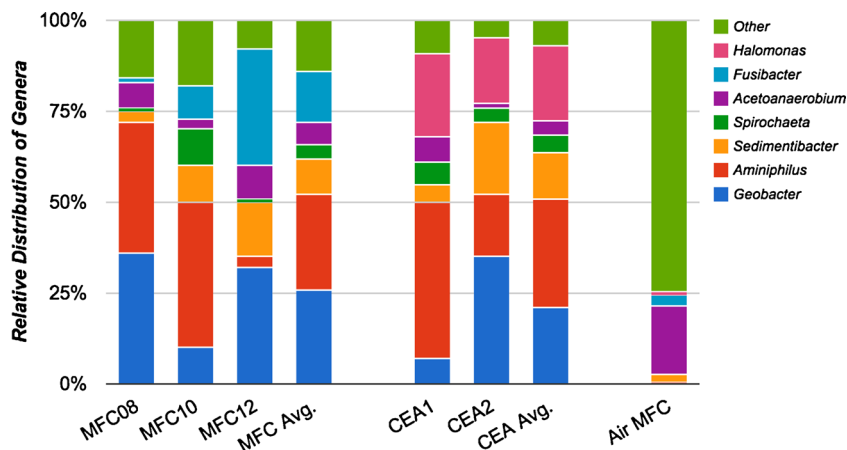


**Fig. 2** Relative distribution of phyla genera all high-power MFCs. MFC08, MFC10, and MFC12 represent communities in SC-MFC reactors from 2008, 2010, to 2012, respectively. CEA1 and CEA2 represent communities in two different CEA-MFC reactors from 2012. Air MFC represents a SC-MFC community exposed to increased airflow



using both UniFrac distance metrics and  $P$  tests (0.05 significance level).

#### Conservation of community across reactor designs

Membership between the dominant constituents of each CEA-MFC community was conserved though there were differences in relative abundances. The CEA2 community had a relative phyla abundance of Proteobacteria double that of CEA1 (51 vs. 25 %). On the other hand, CEA1 had a Synergistetes relative abundance double that of CEA2 (32 vs. 15 %) (Fig. 1). These differences are also reflected on the genus level with CEA1 maintaining a reduced abundance of *Geobacter* (7 vs. 35 %) and *Sedimentibacter* (5 vs. 20 %) populations accompanied by an increase of *Aminiphilus* (43 vs. 17 %) (Fig. 2). Despite these differences, performance was not greatly affected as significant power generation was observed for both reactors (4.3 and 3.4 W m<sup>-2</sup>). There was no significant difference between the two CEA-MFCs using both UniFrac distance metrics and  $P$  tests (0.05 significance level).

Proteobacteria, Firmicutes, Synergistetes, Bacteroidetes, and Spirochaetes were all present in both SC-MFC and CEA-MFC communities with comparable relative abundances. Synergistetes populations were slightly increased in SC-MFCs while higher abundances of Proteobacteria and Firmicutes were seen in CEA-MFCs. The primary difference between the communities from the different reactors was the presence of *Halomonas* (21±4 %) and an absence of *Fusibacter* in CEA-MFC communities. Outside of *Halomonas*, all genera that were present at over 0.5 % of total reads in CEA-MFCs (Table 3) were also present at similar levels in SC-MFCs (Table 2). The large differences in power between SC-MFCs and CEA-MFCs were possibly due to decreased internal resistances rather than the changes in the microbial communities.

It has been proposed that anodic biofilms in CEA-MFC reactors may have to adjust to increased dissolved oxygen levels due to closer proximity to air-exposed cathodes (Fan

et al. 2012). To determine if this may be responsible for the differences in community composition between the two reactor designs, a SC-MFC biofilm was exposed to increased air flow and a dissimilar community structure developed. Abundances of Synergistetes, Bacteroidetes, and Spirochaetes were diminished, making up only a little over 1 % of the oxygen exposed biofilm compared to the 30–40 % found in the other MFC communities. Members of Proteobacteria increased in abundance by roughly twofold though the established exoelectrogen *Geobacter* did not increase but instead saw a sharp decrease in abundance from 26 ±14 % to 0.3 %. A large increase in the aerobic bacterium *Delftia* was observed, composing 33 % of the biofilm. Of those bacteria that were conserved across high-power reactors, only *Acetoanaerobium* remained in significant abundances (19 %) post-oxygen exposure. These results suggest that simply increasing oxygen exposure to the anodic biofilm of a SC-MFC reactor will not shift the community composition toward those seen in CEA-MFCs.

#### Community development during start-up

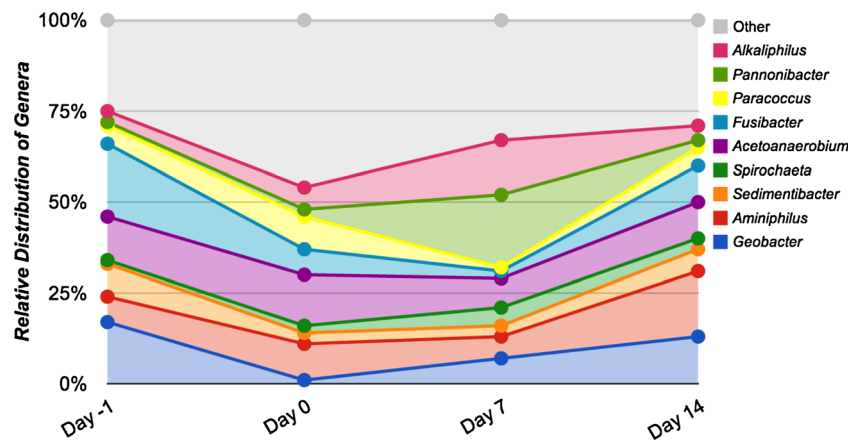
Little variation in community composition was observed on a phylum level over the course of development from the inoculum to a stable high-power community, but there were clear differences on a genus level (Fig. 3). Compared to stable high-power communities (day 1 and day 14), the effluent used as inoculum (day 0) had lower percentages of *Geobacter* (1 vs. 15±3 %), *Sedimentibacter* (3 vs. 8±2 %), and *Fusibacter* (7 vs. 15±7 %). The inoculum contained a larger quantity of bacteria outside the core genera reflected in the large percentage of “other” bacteria. As the biofilm develops, the abundance of other bacteria decreases from 48 % at day 0 to 28 % at day 14. During community development (day 7), both *Pannonibacter* (20 %) and *Alkaliphilus* (15 %) make up a significantly larger percentage of the community compared to the mature communities where they make up 1.50±0.71 % and 3.50±0.71 %, respectively. Additional studies on anode

**Table 2** Core microbiome of acetate-fed SC-MFCs (percent of total 16S rRNA reads)

Phylum	Class	Order	Family	Genus			
Proteobacteria	δ-Proteobacteria	<i>Desulfuromonadales</i>	<i>Geobacteraceae</i>	<i>Geobacter</i>	22.30 %	22.12 %	
		<i>Rhizobiales</i>	<i>Phyllobacteriaceae</i>		1.47 %		
	α-Proteobacteria	<i>Rhodospirillales</i>	<i>Bradyrhizobiaceae</i>			0.83 %	
		<i>Rhodobacteriales</i>	<i>Rhodospirillaceae</i>	<i>Azospirillum</i>		1.46 %	1.14 %
	β-Proteobacteria	<i>Caulobacteriales</i>	<i>Rhodobacteriales</i>	<i>Rhodobacteraceae</i>	<i>Pannonibacter</i>	1.38 %	1.01 %
		<i>Burkholderiales</i>	<i>Caulobacteriales</i>	<i>Caulobacteraceae</i>	<i>Brevundimonas</i>	0.95 %	0.74 %
			<i>Burkholderiales</i>	<i>Comamonadaceae</i>		0.79 %	
			<i>Pseudomonadales</i>	<i>Alcaligenaceae</i>		0.74 %	
	Firmicutes	γ-Proteobacteria	<i>Pseudomonadales</i>	<i>Pseudomonadaceae</i>	<i>Pseudomonas</i>	1.05 %	0.64 %
			<i>Clostridiales</i>	<i>Incertae Sedis XII</i>	<i>Fusibacter</i>	12.46 %	12.38 %
Clostridia		<i>Clostridiales</i>	<i>Incertae Sedis XI</i>	<i>Sedimentibacter</i>		9.68 %	7.80 %
			<i>Peptostreptococaceae</i>	<i>Acetoanaerobium</i>		6.86 %	5.63 %
			<i>Clostridiaceae</i>	<i>Alkaliphilus</i>		2.31 %	1.04 %
			<i>Synergistales</i>	<i>Synergistaceae</i>	<i>Natronincola</i>		0.62 %
Synergistetes	Synergistia	<i>Synergistales</i>			22.13 %	21.14 %	
Spirochaetes	Spirochaetes	<i>Spirochaetales</i>	<i>Spirochaetaceae</i>		3.21 %	0.69 %	
	Bacteroidetes	Bacteroidia	<i>Bacteroidales</i>	<i>Spirochaeta</i>		3.10 %	
Verrucomicrobia	Opitutae						
Actinobacteria	Actinobacteria	<i>Actinomycetales</i>					



**Fig. 3** Relative distribution of genera over the course of development. The initial time point (day 1) represents a stable high-power community; effluent from the high-power MFC was used as inoculum (day 0) and sampled over 2 weeks (day 7/day 14)



study are *Geobacter* spp., *Aminiphilus* spp., *Sedimentibacter* spp., *Acetoanaerobium* spp., and *Spirochaeta* spp. Of all the genera that made up at least 0.5 % of total reads in either SC- or CEA-MFCS, only two, *Halomonas* and *Fusibacter*, were not present in nearly equal abundance in both reactor types. *Halomonas* spp. represented 15.11 % of total reads in CEA-MFC biofilms but was absent in SC-MFC biofilms, while *Fusibacter* was absent in CEA-MFCs but represented 12.38 % of total reads in SC-MFC biofilms. Both have been previously detected in acetate-fed MFC biofilms though their functional roles remain undefined (Erable et al. 2009; Ren et al. 2011). However, those roles may be similar, and the slightly increased salinity of the CEA-MFC media may lead to *Halomonas* filling a specific ecological niche that *Fusibacter* would otherwise fill. It is unlikely that increased oxygen exposure would be responsible for the differences observed between the SC- and CEA-MFC communities.

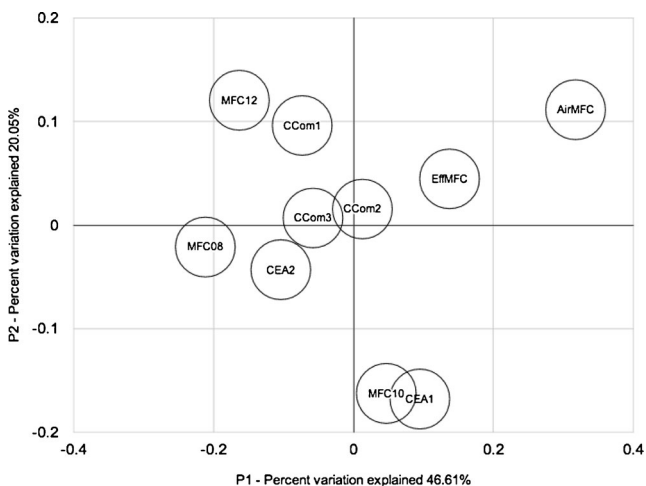


**Fig. 4** Principle components analysis of all MFC communities analyzed includes SC-MFC communities from various years (MFC08, MFC10, and MFC12), CEA-MFC communities (CEA1 and CEA2), an SC-MFC community exposed to increased airflow (air MFC), and combined planktonic and biofilm communities during development (CCom1, EfmMFC, CCom2, and CCom3)

Much of the core microbiome defined here have functional roles within the biofilm community that remain unknown, yet the function of *Geobacter* in these communities has been well explored. *Geobacter* spp. have been utilized as biological models for extracellular electron transfer due to anode-respiring capabilities. *Geobacter* spp. have been shown to develop direct electrical connections with electrodes and may be able to confer conductivity to biofilms (Malvankar et al. 2012, 2011). While *Geobacter* is fairly ubiquitous in anodic biofilms, other similarities between the present community and communities from other studies are limited. Much of this variation in membership between communities is likely due to differences in reactor designs as well as electron donors though some overlap was expected given the ability of many MFC communities to repeatedly converge to stable configurations over relatively short periods of time.

Other similarities observed between this study and previously published MFC community analyses are primarily on a phylum level. Previous studies on MFC anode communities reveal similar phyla-level patterns with four of the five most common phyla in this study also common in similar studies. Proteobacteria consistently make up a large percentage of the bacteria in all MFC biofilms though the secondary and tertiary phyla can vary. Vargas et al. reported Proteobacteria and Bacteroidetes to be far and away the most common phyla, making up 95 % of the biofilm under similar conditions (acetate electron donor, batch mode, and carbon cloth anode) (Vargas et al. 2013). Another study using acetate observed that three phyla (Proteobacteria, Bacteroidetes, and Spirochaetes) composed 92 % of the biofilm, differing from the present findings in the lack of Firmicutes and Synergistetes present (Malvankar et al. 2012). The use of formic acid in place of acetate had no effect on composition on a phyla composition (Kiely et al. 2010). Anode biofilms from an MFC fed with food waste were reported to consist of 41 % Proteobacteria, 40 % Bacteroidetes, and 14 % Firmicutes, with the next two most common phyla being Spirochaetes and Synergistetes (Jia et al. 2013).



While small percentages of Synergistetes are not particularly rare in microbial communities associated with wastewater bioreactors, the large abundances reported here are. Members of the Synergistetes phyla have been detected in anaerobic digesters handling distillery grains, petroleum hydrocarbons, swine wastewater, and even in bioelectrochemical reactors associated with methane fermentation, but not in high numbers (Ducey and Hunt 2013; Sasaki et al. 2013; Scherr et al. 2012; Ziganshin et al. 2011). The genus identified in the present study, *Aminiphilus*, has previously been associated with electrodes among other communities with relative abundances as high as 8.4 and 11 % in PBDE-degrading and hydraulic fracturing wastewaters, respectively (Murali Mohan et al. 2013; Xu et al. 2012). However, relative Synergistetes abundances as high as 33 % and relative *Aminiphilus* abundances as high as 43 % seen in the present study have not previously been reported in any ecological survey.

The contribution of Synergistetes to overall MFC performance is unclear, yet it could relate to the ability of species such as *A. circumscriptus* to efficiently ferment a variety of amino acids (Díaz et al. 2007). Proteins from dead cells may be digested quickly, recycling key nutrients and possibly improving conductivity/electrical interactions with the electrode. Products of amino acid fermentation by *A. circumscriptus* include H<sub>2</sub> as well as acetate, which is the preferred electron donor of *G. sulfurreducens*, hinting at a potential syntrophic interaction. This potential syntrophic interaction between *A. circumscriptus* and *G. sulfurreducens* fits nicely into a model of three-way syntrophy previously proposed for anodic biofilms (Parameswaran et al. 2010). In this model, *Acetoanaerobium* spp., capable of acetate production from H<sub>2</sub> and CO<sub>2</sub>, could conceivably serve the role of the homo-acetogenic hydrogen scavenger (Sleat et al. 1985). Methanogens could also serve a functional role in these communities though community analyses on archaea were not performed. However, it is unlikely that archaea contribute significantly to these communities as previous gas analyses have not revealed methane generation (data unpublished) and high coulombic efficiencies (83.5 %) have been reported (Fan et al. 2012). Previous studies on acetate-fed MFC communities have similarly indicated the presence of very few archaeal sequences (Borole et al. 2009).

A clear, consistent, stable core microbiome is present and identifiable in the communities analyzed as many of the phylogenies are highly conserved. Functional conservation is likely to exist between the microbial communities in this and previous studies and should be further explored, as establishing a core microbiome is an important first step towards understanding the dynamic metabolic processes that occur in these communities and strengthening correlations between community structure, development, and performance. Though significance could be improved by increasing the number of

samples, the present study should be used as point of comparison with future experiments focusing on MFC performance utilizing alternate energy sources and actual waste streams. Variation from the present core community after exposure to varying conditions will be able to offer clues on the functions members identified here serve in their environments as well as the stability of the core community in practical applications. This knowledge may then be applied towards the goal of optimization of these communities, eventually leading to the efficient treatment of waste streams with high-power generation in commercial settings.

**Acknowledgments** We thank Mark Dasenko at the Oregon State University Center for Genome Research and Biocomputing (CGRB) for sequencing support. Research was financially supported by the US National Science Foundation (CBET 0955124).

## References

- Altschul SF, Gish W, Miller W, Myers EW, Lipman DJ (1990) Basic local alignment search tool. *J Mol Biol* 215:403–410. doi:10.1016/S0022-2836(05)80360-2
- Borole AP, Hamilton CY, Vishnivetskaya T, Leak D, Andras C (2009) Improving power production in acetate-fed microbial fuel cells via enrichment of exoelectrogenic organisms in flow-through systems. *Biochem Eng J* 48:71–80. doi:10.1016/j.bej.2009.08.008
- Borole AP, Hamilton CY, Vishnivetskaya TA (2011) Enhancement in current density and energy conversion efficiency of 3-dimensional MFC anodes using pre-enriched consortium and continuous supply of electron donors. *Bioresour Technol* 102:5098–5104. doi:10.1016/j.biortech.2011.01.045
- Cole JR, Wang Q, Cardenas E, Fish J, Chai B, Farris RJ, Kulam-Syed-Mohideen AS, McGarrell DM, Marsh T, Garrity GM, Tiedje JM (2009) The Ribosomal Database Project: improved alignments and new tools for rRNA analysis. *Nucleic Acids Res* 37:D141–D145. doi:10.1093/nar/gkn879
- Díaz C, Baena S, Fardeau M-L, Patel BKC (2007) *Aminiphilus circumscriptus* gen. nov., sp. nov., an anaerobic amino-acid-degrading bacterium from an upflow anaerobic sludge reactor. *Int J Syst Evol Microbiol* 57:1914–1918. doi:10.1099/ijs.0.63614-0
- Ducey TF, Hunt PG (2013) Microbial community analysis of swine wastewater anaerobic lagoons by next-generation DNA sequencing. *Anaerobe* 21:50–57. doi:10.1016/j.anaerobe.2013.03.005
- Edgar RC (2004) MUSCLE: multiple sequence alignment with high accuracy and high throughput. *Nucleic Acids Res* 32:1792–1797. doi:10.1093/nar/gkh340
- Erable B, Roncato M-A, Achouak W, Bergel A (2009) Sampling natural biofilms: a new route to build efficient microbial anodes. *Environ Sci Technol* 43:3194–3199. doi:10.1021/es803549v
- Fan Y, Hu H, Liu H (2007) Enhanced Coulombic efficiency and power density of air-cathode microbial fuel cells with an improved cell configuration. *J Power Sources* 171:348–354. doi:10.1016/j.jpowsour.2007.06.220
- Fan Y, Sharbrough E, Liu H (2008) Quantification of the internal resistance distribution of microbial fuel cells. *Environ Sci Technol* 42:8101–8107. doi:10.1021/es801229j
- Fan Y, Han S-K, Liu H (2012) Improved performance of CEA microbial fuel cells with increased reactor size. *Energy Environ Sci* 5:8273. doi:10.1039/c2ee21964f

- Franks AE, Nevin K (2010) Microbial fuel cells, a current review. *Energies* 3:899–919
- Hamady M, Lozupone C, Knight R (2010) Fast UniFrac: Facilitating high-throughput phylogenetic analyses of microbial communities including analysis of pyrosequencing and PhyloChip data. *ISME J* 4:17–27. doi:10.1038/ismej.2009.97
- Ishii S, Watanabe K, Yabuki S, Logan BE, Sekiguchi Y (2008) Comparison of electrode reduction activities of *Geobacter sulfurreducens* and an enriched consortium in an air-cathode microbial fuel cell. *Appl Environ Microbiol* 74:7348–7355. doi:10.1128/AEM.01639-08
- Jia J, Tang Y, Liu B, Wu D, Ren N, Xing D (2013) Electricity generation from food wastes and microbial community structure in microbial fuel cells. *Bioresour Technol* 144:94–99. doi:10.1016/j.biortech.2013.06.072
- Kiely PD, Call DF, Yates MD, Regan JM, Logan BE (2010) Anodic biofilms in microbial fuel cells harbor low numbers of higher-power-producing bacteria than abundant genera. *Appl Microbiol Biotechnol* 88:371–380. doi:10.1007/s00253-010-2757-2
- Kiely PD, Regan JM, Logan BE (2011) The electric picnic: synergistic requirements for exoelectrogenic microbial communities. *Curr Opin Biotechnol* 22:378–385. doi:10.1016/j.copbio.2011.03.003
- Kuczynski J, Costello EK, Nemergut DR, Zaneveld J, Lauber CL, Knights D, Koren O, Fierer N, Kelley ST, Ley RE, Gordon JI, Knight R (2010) Direct sequencing of the human microbiome readily reveals community differences. *Genome Biol* 11:210. doi:10.1186/gb-2010-11-5-210
- Lee T, Van Doan T, Yoo K, Choi S, Kim C, Park J (2010) Discovery of commonly existing anode biofilm microbes in two different wastewater treatment MFCs using FLX Titanium pyrosequencing. *Appl Microbiol Biotechnol* 87:2335–2343. doi:10.1007/s00253-010-2680-6
- Liu H, Logan BE (2004) Electricity generation using an air-cathode single chamber microbial fuel cell in the presence and absence of a proton exchange membrane. *Environ Sci Technol* 38:4040–4046. doi:10.1021/es0499344
- Logan BE (2008) *Microbial fuel cells*. Wiley
- Malvankar NS, Lau J, Nevin KP, Franks AE, Tuominen MT, Lovley DR (2012) Electrical conductivity in a mixed-species biofilm. *Appl Environ Microbiol* 78:5967–5971. doi:10.1128/AEM.01803-12
- Malvankar NS, Vargas M, Nevin KP, Franks AE, Leang C, Kim B-C, Inoue K, Mester T, Covalla SF, Johnson JP, Rotello VM, Tuominen MT, Lovley DR (2011) Tunable metallic-like conductivity in microbial nanowire networks. *Nat Nanotechnol* 6:573–579. doi:10.1038/nnano.2011.119
- Murali Mohan A, Hartssock A, Hammack RW, Vidic RD, Gregory KB (2013) Microbial communities in flowback water impoundments from hydraulic fracturing for recovery of shale gas. *FEMS Microbiol Ecol*. doi:10.1111/1574-6941.12183
- Parameswaran P, Zhang H, Torres CI, Rittmann BE, Krajmalnik-Brown R (2010) Microbial community structure in a biofilm anode fed with a fermentable substrate: the significance of hydrogen scavengers. *Biotechnol Bioeng* 105:69–78. doi:10.1002/bit.22508
- Potter MC (1911) Electrical effects accompanying the decomposition of organic compounds. *Proc R Soc Lond Ser B Contain Pap Biol Character* 84:260–276
- Ren Z, Ramasamy RP, Cloud-Owen SR, Yan H, Mench MM, Regan JM (2011) Time-course correlation of biofilm properties and electrochemical performance in single-chamber microbial fuel cells. *Bioresour Technol* 102:416–421. doi:10.1016/j.biortech.2010.06.003
- Sasaki D, Sasaki K, Watanabe A, Morita M, Matsumoto N, Igarashi Y, Ohmura N (2013) Operation of a cylindrical bioelectrochemical reactor containing carbon fiber fabric for efficient methane fermentation from thickened sewage sludge. *Bioresour Technol* 129:366–373. doi:10.1016/j.biortech.2012.11.048
- Scherr KE, Lundaa T, Klose V, Bochmann G, Loibner AP (2012) Changes in bacterial communities from anaerobic digesters during petroleum hydrocarbon degradation. *J Biotechnol* 157:564–572. doi:10.1016/j.jbiotec.2011.09.003
- Schloss PD, Westcott SL, Ryabin T, Hall JR, Hartmann M, Hollister EB, Lesniewski RA, Oakley BB, Parks DH, Robinson CJ, Sahl JW, Stres B, Thallinger GG, Van Horn DJ, Weber CF (2009) Introducing mothur: open-source, platform-independent, community-supported software for describing and comparing microbial communities. *Appl Environ Microbiol* 75:7537–7541. doi:10.1128/AEM.01541-09
- Shade A, Handelsman J (2012) Beyond the Venn diagram: the hunt for a core microbiome. *Environ Microbiol* 14:4–12. doi:10.1111/j.1462-2920.2011.02585.x
- Sleat R, Mah RA, Robinson R (1985) *Acetoanaerobium noterae* gen. nov., sp. nov.: an anaerobic bacterium that forms acetate from H<sub>2</sub> and CO<sub>2</sub>. *Int J Syst Bacteriol* 35:10–15. doi:10.1099/00207713-35-1-10
- Turnbaugh PJ, Ley RE, Mahowald MA, Magrini V, Mardis ER, Gordon JI (2006) An obesity-associated gut microbiome with increased capacity for energy harvest. *Nature* 444:1027–131. doi:10.1038/nature05414
- Vargas IT, Albert IU, Regan JM (2013) Spatial distribution of bacterial communities on volumetric and planar anodes in single-chamber air-cathode microbial fuel cells. *Biotechnol Bioeng*. doi:10.1002/bit.24949
- Wang X, Hu M, Xia Y, Wen X, Ding K (2012) Pyrosequencing analysis of bacterial diversity in 14 wastewater treatment systems in China. *Appl Environ Microbiol* 78:7042–7047. doi:10.1128/AEM.01617-12
- Xu M, Chen X, Qiu M, Zeng X, Xu J, Deng D, Sun G, Li X, Guo J (2012) Bar-coded pyrosequencing reveals the responses of PBDE-degrading microbial communities to electron donor amendments. *PLoS ONE* 7:e30439. doi:10.1371/journal.pone.0030439
- Yates MD, Kiely PD, Call DF, Rismani-Yazdi H, Bibby K, Peccia J, Regan JM, Logan BE (2012) Convergent development of anodic bacterial communities in microbial fuel cells. *ISME J* 6:2002–2013. doi:10.1038/ismej.2012.42
- Yi H, Nevin KP, Kim B-C, Franks AE, Klimes A, Tender LM, Lovley DR (2009) Selection of a variant of *Geobacter sulfurreducens* with enhanced capacity for current production in microbial fuel cells. *Biosens Bioelectron* 24:3498–3503. doi:10.1016/j.bios.2009.05.004
- Zhang G, Zhao Q, Jiao Y, Wang K, Lee D-J, Ren N (2012) Efficient electricity generation from sewage sludge using biocathode microbial fuel cell. *Water Res* 46:43–52. doi:10.1016/j.watres.2011.10.036
- Ziganshin AM, Schmidt T, Scholwin F, Il'inskaya ON, Harms H, Kleinstaub S (2011) Bacteria and archaea involved in anaerobic digestion of distillers grains with solubles. *Appl Microbiol Biotechnol* 89:2039–2052. doi:10.1007/s00253-010-2981-9